ESO Phase 3 Data Release Description

Data Collection	ERIS/NIX Imager
Author	Mark Neeser
Data Provider	Isabelle Percheron
Document Date	2024.07.17
Document Version	1.1

Abstract

This is the release of the reduced imaging data from the ERIS/NIX instrument from the beginning of operations on April 1, 2023 (P111).

The **E**nhanced **R**esolution **I**mager and **S**pectrograph (**ERIS**) is a general-use infrared imager (NIX) and integral field spectrograph (SPIFFIER) that utilises the adaptive optics on the VLT's Unit Telescope 4 (Yepun)[1]. NIX operates in the near-infrared range of 1 – 5 μm (J to Mp bands) and is designed to provide diffraction limited imaging[2]. The focus of this release is dedicated to the fully reduced products from the ERIS/NIX imager with the 13 or 27mas/pixel cameras (field-of-view of 27"x27" and 55"x55"). The other modes and data formats offered by NIX, coronagraphy, very short exposure "burst" mode cubes, and long-slit spectroscopy are currently not included in this release, but may be added at a later date.

The NIX data consists of science exposures that have been dark-corrected, flat-fielded, linearity and gain corrected, sky background corrected, and astrometrically and photometrically calibrated. The data provided consists of combined (stacked), resampled exposures, their associated single-band source detection catalogues, and the individual exposures that make up the stacked images. Each of these frames is provided as a multi-extension fits file.

General information and ERIS/NIX processing

Overview of Observations

This data set contains all of the science observations done using the ERIS/NIX imaging instrument. These are not part of a single self-contained project or survey. Rather, they contain observations from many different projects and surveys, using various filters and observing methods. The distribution of fields is obviously governed by the time of year in which the observations were taken.

Release Content

This release contains all of the science observations done with ERIS since it began operations starting from April 2023 (period P111). New data products are being continuously created and are added at regular intervals.

This release also includes data processed from the ERIS/NIX Science Verification observations made from December 2 – 5, 2022 (https://www.eso.org/sci/activities/vltsv/erissv.html). Here, all proposals with "completed" or "partially completed" data status have been processed.

---

[1] https://www.eso.org/sci/facilities/paranal/instruments/eris.html
[2] https://www.eso.org/sci/facilities/paranal/instruments/eris/inst.html

For science observations the following data products are available:

- Resampled and combined (stacked) jittered images.

- Single-band source catalogues for the stacks

- All of the individual exposures that make up the stacked images.

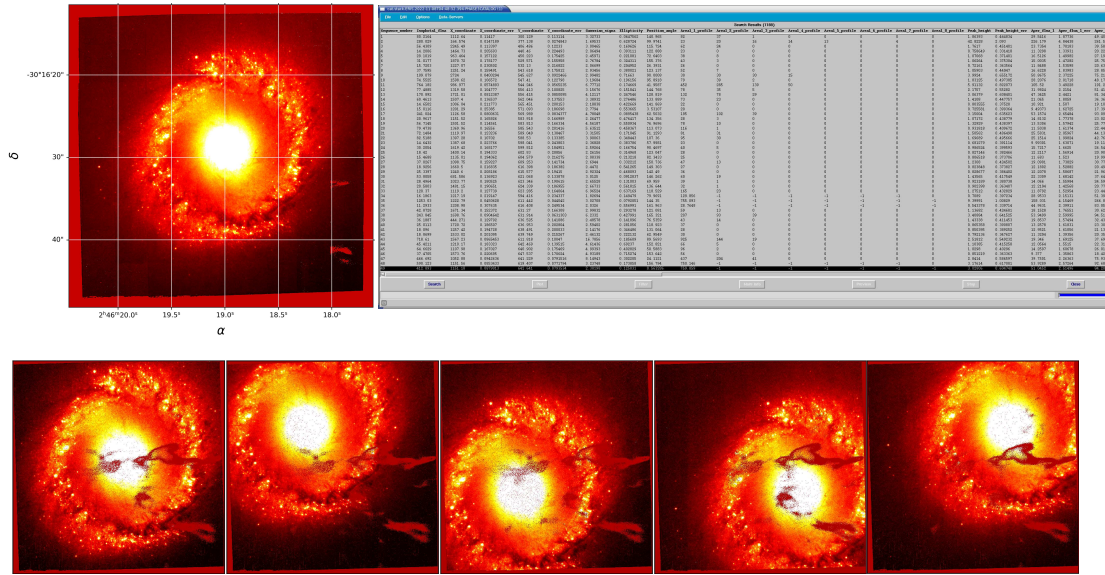All reduction has been done at the OB level and no attempt has been made to combine data between multiple OB's.

Figure 1: an example of the science image data products provided in this release. Clockwise from the top left are the stacked jittered images, the source catalogue from the image stack, and the individual exposures that make up the stack.

The following observations have been omitted from this release:
- Observations done under any technical programme having an OBS.PROG.ID like "60" and "060" (including any standard star observations).
- Observations done in ERIS/NIX cube mode (DPR.CATG = SCIENCE and DPR.TECH = IMAGE and DET.FRAM.FORMAT=cube).
- Coronographic observations (DPR.CATG = SCIENCE and DPR.TECH = CORONAGRAPHY,APP).
- Long slit spectra (DPR.CATG = SCIENCE and DPR.TECH = SPECTRUM,LSS or DPR.TECH=SPECTRUM,LSS,JITTER).

Release Notes

The data for this release was processed using the ERIS/NIX science pipeline developed by UKATC Edinburgh (John Lightfoot) and by ESO. The main processing steps are described in the following section.

Data Reduction and Calibration

For all science observations the following data reduction steps are performed:

- Each image is dark-corrected using a master dark frame of the correct DIT/NDIT combination. By and large dark observations are done after sunrise for the DIT/NDIT combinations that have been used during the previous night. Where this has not been the case or where there was some sort of failure in the dark observation, a similar master dark frame from another night has been substituted.
- A linearization and gain correction is applied based on an associated, dedicated linearity calibration series.
- Flat fielding is done using a master flat created from a lamp flat and a sky or twilight flat for the matching filter. The lamp flat contributes the high signal-to-noise pixel-to-pixel variations (high frequency component) while the sky flat contributes the large scale variations (low frequency component).
- A sky background estimate is obtained and subtracted from each individual exposure. Getting this correct is just about the hardest task in infrared imaging. If in the input processing there are sky frames provided (JITTER_SKY) then the sky will be estimated from them and the result used for all object frames. Otherwise, the sky is estimated from the target jittered frames themselves. The basic idea is to stack the jittered object images without resampling onto common sky coordinates so that any objects 'move about' over the stack pixels. In this situation pixel measurements contaminated by source emission will be outliers from the stack and can be rejected. The sky emission estimate is the mean of the stack after the rejections are complete.
- A source catalogue is extracted for each exposure and this is used to fit a world coordinate system (WCS). The TAN projection is used in conjunction with known projection coefficients that provide an initial WCS refinement based on the pixel scale and rotation measured at the 13 and 27mas pixel scales. The WCS is generally computed between *in situ* sources matched to the GAIA DR3 source catalogue. If, however, there are too few GAIA sources available in the small field of view ERIS images, then the sources in the first image are matched to the remaining images of the OB, and only the relative offsets between the exposures are mapped. The WCS is then simply that provided by the telescope. This results in a good relative overlap between all of the input exposures, but the absolute astrometry can then be poor. See Appendix 1 for a further discussion of this case.
- The individual exposures for a single OB and a given detector are stacked using the WCS solutions defined above or, in the case of too few reference stars, the relative image-to-image offsets. The stacks are formed using a *drizzle* interpolation algorithm to resample the input pixels onto the output grid. This leads to an OB stack for each science exposure.
- For each individual science exposure a match of the source extraction catalogue is also done using the 2MASS catalogue. If sufficient *in situ* 2MASS sources exist, then these are used to compute a zeropoint for the frame. This is currently only possible for the J, H, and Ks wavebands. At the moment, it is assumed that the 2MASS and ERIS/NIX filter/detector responses are identical and no colour-colour transformations are included. This is an ongoing project and will be applied to the data when available.
  If an insufficient number of 2MASS sources exist in the image a filter default zeropoint value is used based on an analysis of a large number of ERIS/NIX standard star exposures (see Appendix 2).
  Which of two photometric calibration methods was used can be determined from the image keywords:
  ZPMETHOD = 2MASS   (If the zeropoint has been computed using *in situ* 2MASS stars)
  ZPMETHOD = DEFAULT (If the zeropoint has been estimated using filter default values)
- Finally, a single-band source detection catalogue is extracted from the stacked images.
- The spatial resolution quality keyword PSF_FWHM is computed using stellar sources in each image. If there are an insufficient number of stars in the field of view and AO is used, then the image PSF_FWHM is computed using the attached ASM_DATA table. The

image quality is then measured from the Shack-Hartmann wavefront sensor. Otherwise, the Paranal seeing monitor (DIMM) is used by converting its value to the different telescope size, the different waveband, and an average over the duration of the exposure.

All image products are accompanied by a variance map that has been propagated through the complete data reduction process. Each image product also includes a quality map (comprising the hot and cold bad pixels, non-linear pixels, and saturated pixels), as well as a confidence map.

Data Quality

Master calibrations. All master calibrations used to process ERIS/NIX images have been quality-reviewed and certified at the time of acquisition, as part of the closed QC loop with the Observatory which also includes trending. As part of the certification process for calibration data there is a scoring process to bring non-compliant behaviour of the calibrations to the attention of the QC scientist. All these cases have been handled as part of the certification procedure. Hence, there is reasonable evidence that the master calibrations catch all instrument properties, as relevant for the reduction, correctly and completely.

Astrometric Correction

A source catalogue is extracted for each science exposure and this is used to fit a world coordinate system (WCS). When possible, the WCS is computed between *in situ* sources matched to the GAIA DR3 source catalogue. When adequate numbers of GAIA DR3 sources are available in the ERIS/NIX fields, the absolute astrometric solutions are generally better than 300 milliarcseconds.
From this measurement of the astrometric quality it is apparent that these results are slightly worse than the internal errors of the GAIA DR3 catalogue. The slightly larger mean internal rms (σ = +/- 0.26 arcsec) can be explained by two primary reasons. First, the brightest catalogue stars are often saturated in the ERIS/NIX images and, therefore, only the fainter, less reliable, catalogue stars are available for calibration. Secondly, the ERIS adaptive optics uses either a single natural guide star or a single laser generally located near the field centre. This results in an axially symmetric image distortion toward the field edges, in which the stellar sources can appear slightly elongated when furthest away from the NGS or LGS.

If, however, there are too few GAIA sources (generally three stars or less) available in the field-of-view of the ERIS image, then the sources in the first image are matched to the remaining images of the OB, and only the relative offsets between the exposures are mapped. The absolute astrometric solution is then simply the WCS provided by the telescope. This generally results in a good relative overlap between all of the input exposures, but the absolute astrometry can then be as poor as σ = +/- 2 arcsec. It is important to note that due to the small field-of-view of the ERIS/NIX imager (55" x 55" and 27" x 27") it is not uncommon to have an inadequate number of astrometric calibrators. See Appendix 1 for a further discussion of this case.
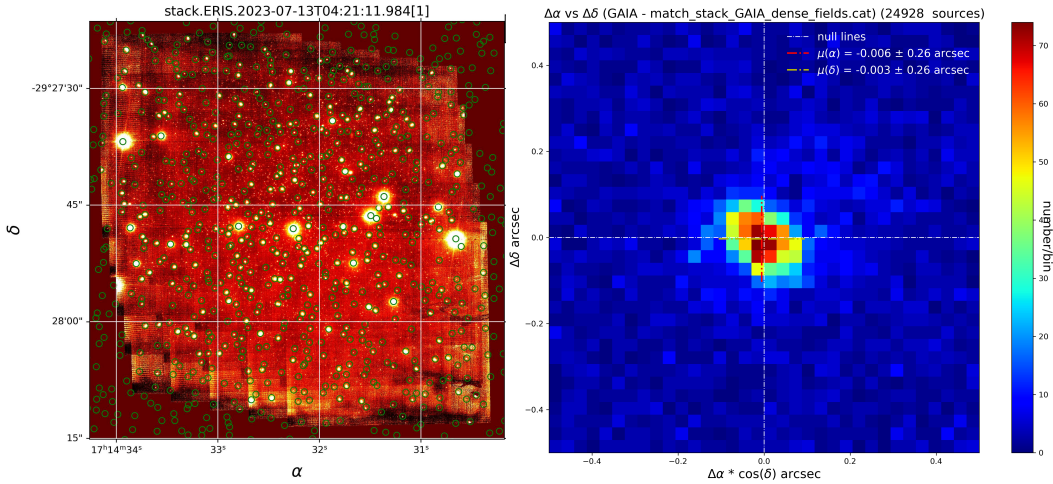
Figure 2: left-panel: an example ERIS/NIX stacked mosaic science image (NGC 6304 in the Ks-band) with a large number of GAIA DR3 sources used for its in situ astrometric calibration. Right-panel: the $\Delta\alpha*\cos(\delta)$ and $\Delta\delta$ offsets between ~25k matched GAIA -- NIX sources as measured in 22 random ERIS/NIX images that have adequate numbers of *in situ* astrometric calibrators. Note that this plot measures 1 arcsec on each side. The standard deviation of this matched distribution (σ = +/-0.26 arcsec) defines the best-case absolute astrometric solution.

Photometric Correction

For the J, H, and Ks filters, the source catalogue extracted for each science exposure is matched to the 2MASS source catalogue and an *in situ* photometric calibration is done when an adequate number of unsaturated 2MASS sources are available.

Currently, we are assuming a one-to-one match between the ERIS/NIX detector and filter bandpasses and those of 2MASS. A project is on-going to map the colour-colour terms for each ERIS filter, by regular observations of 2MASS touchstone fields. When completed, the ERIS/NIX pipeline and archive data photometric calibration will be updated. Until this is done, we are assuming an error of roughly +/- 0.5 magnitudes in the J, H, and Ks filters. For the other ERIS/NIX filters not covered by 2MASS, this error will be larger.

If an inadequate number of 2MASS stars are available in the ERIS/NIX science field, and a photometric standard star observation in the same filter and instrument mode is made during the same night, then this is used to determine the image zeropoint, following a correction of the differences in airmass and apertures between the two images. If neither 2MASS stars or a suitable photometric standard star observation are available, then a default zeropoint for the given filter is used. When this is done, the header keyword ZPMETHOD = DEFAULT. A description of the default zeropoints is given in Appendix 2.

Known issues

The small field of view available with the three ERIS/NIX cameras (55" x 55" and 27" x 27") can often make *in situ* astrometric or photometric calibration challenging. The issues that this creates and the solutions are described in detail in Appendix 1 and Appendix 2.

The weakest attribute of this data release of ERIS images lies in its photometry.
The necessity of photometrically calibrating the science images using default zeropoints, when saufficient numbers of *in situ* catalogue calibrators are not available, is only a "best guess". Furthermore, even with sufficient 2MASS stars in the field, the zeropoint is only an estimate since a full colour-colour transformation between 2MASS and ERIS is still pending. We have assumed that the match between the two filter sets is perfect. This will be improved on in a future data release. Therefore, we recommend that the user treat the ERIS photometry with a degree of caution, or consider refining our zeropoint estimates with further catalogue comparisons (i.e. 2MASS, or further dedicated secondary standard star observations) if a higher level of photometric accuracy is required.

Data Format

Files Types

The data set for each science observation consists of two primary product files (the stacked/jittered image and the source extraction catalogue), one type of ancillary fits files (the processed individual exposures) and one preview plot. The number of ancillary files depends on how many frames were taken on the target during the observation.

- Stacked/jittered images:
  This is delivered as a multi-extension fits file (MEF) that consists of the following image data planes:
  1. the stacked image data
  2. the associated error map propagated through the processing steps
  3. the data quality map
  4. the confidence map

- Single-band source extraction catalogues for the stacks

- Images of all of the individual exposures that make up the stacked images. Each individual science exposure is a multi-extension fits file that consists of the following planes:
  1. the image data
  2. the associated error map
  3. the data quality map
  4. the confidence map
  5. the background map
  6. the error in the background map
  7. the background confidence map

ORIGFILE begins with	Type	Product category HIER-ARCH.ESO.PRO.CATG and PRODCATG	Num-ber	Primary or ancillary?	Description
ER_SCOM	fits	IMG_OBS_COMBINED SCI-ENCE.IMAGE	1	Primary	Stacked/jittered combined image
ER_SCAT	fits	IMG_OBS_CATALOGUE SCIENCE.SRCTBL	1	Primary	Source catalogue for the combined image
ER_SPHO	fits	CAL_PHOT_OBJECT_JITTER	n	Ancillary	Individual expo-sures
	png		1	Ancillary	Preview image (single frames)

Table 1. Primary and ancillary products for a science observation

The ORIGFILE product names for the primary products (ER_SCOM and ER_SCAT) follow a naming convention which is:

```
ER_<TYPE>_<OBS_ID>_<DP_ID>_<ARM>_<TARGET>.fits
```

The ORIGFILE product name for the ancillary product (ER_SPHOT) follows the same naming conven-

tion than the primary products with the addition of <N> which is the exposure number in the template:

```
ER_<TYPE>_<OBS_ID>_<DP_ID>_<ARM>_<TARGET>_<N>.fits
```

Table 2 gives more details on the ORIGFILE naming convention.

In addition to the fits products, also a preview plots is delivered as ancillary file. It comes in the PNG image format and follow the naming convention:

r.ERIS.<DP_ID>_single.png

Component	Description
ER	ERIS product
<TYPE>	Product type. See Table 1.
<OBS_ID>	OB ID of the observation (header key HIERACH ESO OBS ID)
<DP_ID>	Time stamp in UT of the first exposure of the stack in the format <YEAR>-<MONTH>-<DAY>T<HOUR>:<MINUTE>:<SECOND>.<MILLISECOND>
<TARGET>	Coding of HIERARCH.ESO.OBS.TARG.NAME
<N>	HIERACH.ESO.TPL.EXPNO

Table 2. ORIGFILE naming convention

File structure and size

The primary science products as well as the ancillary fits files have a size less than 150MB .

The primary ERIS combined image (PRO.CATG = IMG_OBS_COMBINED) is a fits file with several extensions (see Table 3)

Extension	Description
Primary	Header
DATA	Data image
ERROR	Error Map
DQ	Data quality Map (0,1)
CONFIDENCE	Confidence Map

Table 3. description of the combined product (IMG_OBS_COMBINED)

Catalogue Columns

Table 4: A description of ERIS/NIX catalogue columns

Col #	Name	Description
1	Sequence_number	Running number for ease of reference, in strict order of image detections
2	Isophotal_flux	Standard definition of summed flux within detection isophote.
3	X_coordinate	The x, y coordinates and errors with (1, 1) defined to be the centre of the first active pixel in the image array.
4	X_coordinate_err	
5	Y_coordinate	
6	Y_coordinate_err	
7	Gaussian_sigma	Second moment parameters
8	Ellipticity	
9	Position_angle	
10	Areal_1_profile	The number of pixels above a series of threshold levels, relative to local sky. The levels are set at T, 2T, 4T, 8T, 16T, 32T, 64T and 128T where T is the analysis threshold
11	Areal_2_profile	
12	Areal_3_profile	
13	Areal_4_profile	
14	Areal_5_profile	
15	Areal_6_profile	
16	Areal_7_profile	
17	Areal_8_profile	
18	Peak_height	Peak intensity and its error in ADU relative to local value of sky
19	Peak_height_err	
20	Aper_flux_1	Flux and error within a specified radius aperture, typically set so that $R_{aperture} = \langle FWHM \rangle$ where the quantity in angle brackets is the mean FWHM of all stellar images. This is also known as the "core radius". The apertures here correspond to $(0.5, 1/\sqrt{2}, 1, \sqrt{2}, 2, 2\sqrt{2}, 4, 5, 6, 7, 8, 10,$ and $12)$ times the core radius.
21	Aper_flux_1_err	
22	Aper_flux_2	
23	Aper_flux_2_err	
24	Aper_flux_3	
25	Aper_flux_3_err	
26	Aper_flux_4	
27	Aper_flux_4_err	
28	Aper_flux_5	
29	Aper_flux_5_err	
30	Aper_flux_6	
31	Aper_flux_6_err	
32	Aper_flux_7	
33	Aper_flux_7_err	
34	Aper_flux_8	
35	Aper_flux_8_err	
36	Aper_flux_9	
37	Aper_flux_9_err	
38	Aper_flux_10	
39	Aper_flux_10_err	
40	Aper_flux_11	
41	Aper_flux_11_err	
42	Aper_flux_12	
43	Aper_flux_12_err	
44	Aper_flux_13	
45	Aper_flux_13_err	
46	Petr_radius	Petrosian radius, r_p in pixels as defined in Yasuda, et al. 2001, AJ, 112, 1104.
47	Kron_radius	Kron radius, r_k in pixels as defined by Bertin and Arnouts 1996, A & A Supp, 117, 393.
48	Hall_radius	Hall radius, r_h in pixels as defined by Hall and Mackay 1984, MNRAS, 210, 979.

49	Petr_flux	Petrosian flux and error to $2r_p$
50	Petr_flux_err	
51	Kron_flux	Kron flux and error to $2r_k$
52	Kron_flux_err	
53	Hall_flux	Hall flux and error to $5r_h$. Alternative total flux
54	Hall_flux_err	
55	Error_bit_flag	Bit pattern listing various processing error flags. Currently this is the number of bad pixels included in the aperture flux (Aper_flux_3)
56	Sky_level	Local interpolated sky level from background tracker
57	Sky_rms	Local estimate of variation in sky level around images
58	Parent_or_child	Flag for parent or part of de-blended deconstruct
59	RA	RA and Dec of each object in degrees
60	Dec	

61	Classification	simple flag indicating most probable classification for object:
		    -2: Object is compact (maybe stellar)
		    -1: Object is stellar
		     0: Object is noise
		     1: Object is non-stellar

62	Statistic	an equivalent N(0,1) measure of how stellar-like an image is. It is used in deriving the classification in a "necessary but not sufficient" sense. This statistic is computed from a discrete curve-of-growth analysis from the peak and aperture fluxes and also factors in ellipticity information. The stellar locus is used to define the "mean" and "sigma" as a function of magnitude such that the "statistic" can be normalised to an approximate N(0,1) distribution.
63-80	blank	

Converting the source catalogue fluxes (here, using any of the 13 aperture flux values: Aper_flux_1 to Aper_flux_13) to magnitudes can be done with the following relation:

$$\text{magnitude} = \text{PHOTZP} - 2.5 * \log_{10}(\text{Aper\_flux\_i}) - \text{APCORi} \qquad (\text{for } i = 1 \ldots 13)$$

where uppercase parameters indicate header keywords:

PHOTZP   = the photometric zeropoint [magnitude]
APCORi   = the stellar aperture correction for i^{th} aperture flux [magnitude]
                (this keyword can be found in the source catalogue file)

Acknowledgement text

Appendix 1: Astrometric Correction

The ERIS/NIX pipeline generally uses GAIA sources in the field of each science exposure to create an astrometric plate solution. However, this is not always be possible. The relatively small fields of ERIS/NIX (57" × 57" and 27" × 27"), implies that some pointings will have too few GAIA sources to allow an automatic improvement of the frame's absolute world coordinate system (WCS). An investigation was done to estimate the probability of any given ERIS/NIX field having N GAIA sources. For both ERIS field sizes, approximately 4.5×10^6 pointings were randomly distributed in a range of right ascension and declination accessible to Paranal. For each such pointing, the DR3 GAIA catalogue was queried and the number of GAIA sources counted.

As is expected, the density of GAIA sources is greatest near the Galactic plane and declines rapidly at high Galactic latitudes. However, because of the small field of ERIS it is possible to have zero GAIA sources at almost any value of Galactic longitude or latitude (see figure 3). As can be seen in figure 4 a full 26% of all random ERIS/NIX pointings will have no GAIA sources in the field. For the 27"× 27" this is significantly worse and more than one half of the fields will have no GAIA sources. Since the pipeline will require three or more good GAIA catalogue sources to correlate with detections in the ERIS image, the situation can be considerably worse. In cases such as these, the ERIS/NIX pipeline will compute relative offsets from the reference frame in the OB jitter and will use the absolute WCS given by the telescope. In this way, the relative matching between the frames of the OB can be good, however, the absolute astrometry can be off by several arcseconds.
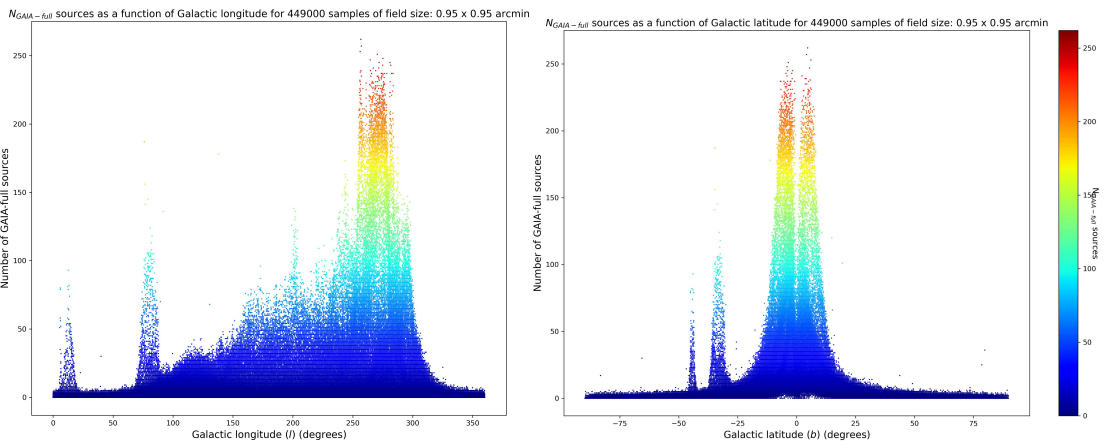

Figure 3: The number of GAIA sources in a random distribution of 4.5×10^6 ERIS/NIX pointings with a field-of-view of 57" × 57" as a function of Galactic longitude (left panel) and latitude (right panel). The density of GAIA sources is obviously greatest near the Galactic plane and declines rapidly at high Galactic latitudes. However, the small field of ERIS implies that it is possible to have zero GAIA sources at any value of (l, b).
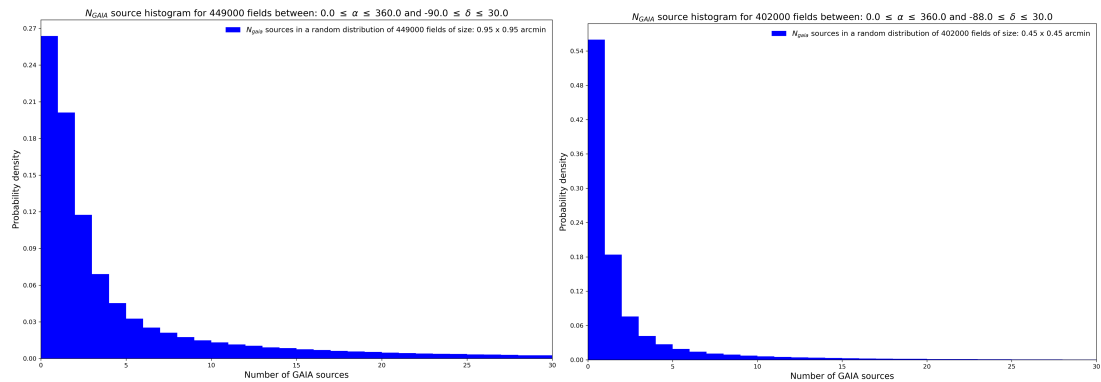

Figure 4: The distribution of ERIS/NIX pointings with a 57" × 57" field-of-view (left panel) and 27" × 27" field-of-view (right panel) having 0 to 30 GAIA sources.

Appendix 2: Default Zeropoints for ERIS/NIX Filters

Default zeropoints are used as a fall-back solution to calibrate the photometry of ERIS/NIX images. If there are an insufficient number of 2MASS stars in the field with which to do an in situ photometric calibration, or when a separate standard star has not been obtained in the same filter configuration, then a default zeropoint is used. In this case, the PHOTZP keyword is assigned the default value for the given filter. When this is done the header keyword:

ZPMETHOD = DEFAULT   'ZP computed from filter default value'

To compute default zeropoints for all ERIS/NIX filters, the standard stars images (TPL_ID = *ERIS_nixIMG_cal_StandardStar*) observed between April 01, 2023 and February 7, 2024 were processed. These 904 standard star exposures were made in the J, H, Ks, Lp, and Mp bandpasses.

Zeropoint computation

For each filter all available images (PRO.CATG = CAL_PHOT_OBJECT_JITTER) and associated source catalogues (PRO.CATG = CAL_PHOT_CATALOGUE) are matched to the target standard (OBS.TARG.NAME) and the photometric zeropoint is computed using:

$$\text{PHOTZP} = \text{magnitude\_STD} - 2.5 * \log_{10}(\text{Aper\_flux\_7}) - \text{APCOR7}$$

where:

mag_STD   =   the standard star magnitude in the given bandpass
Aper_flux_7 =   the catalogue flux value with aperture $R_{aperture} = 4.* \langle FWHM \rangle$
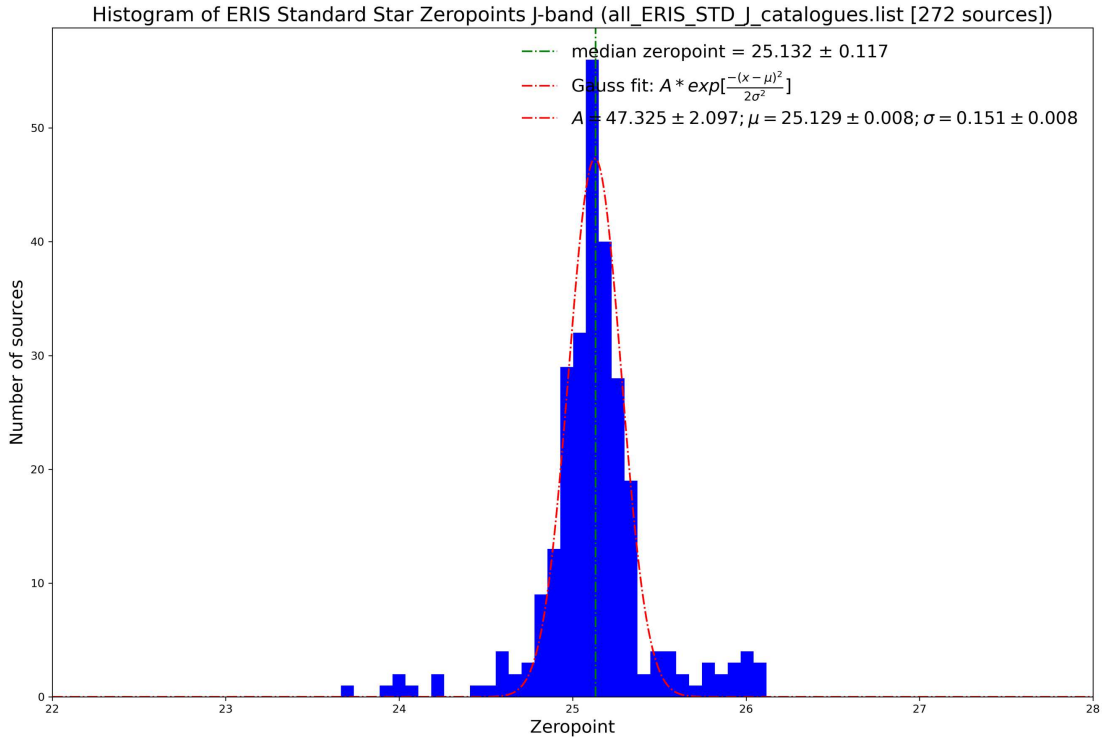APCOR7   =   stellar aperture correction for Aper_flux_7.

Figure 5: The zeropoint distribution of 272 J-band standard stars. A Gaussian fit provides the mean default zeropoint and its standard deviation its associated error. Similar plots for H, Ks, Lp, and Mp provide the zeropoints for those filters. For the remaining ERIS/NIX narrow-band filters an estimate is made by using the nearest, overlapping broad band filter for which the zeropoint is known.
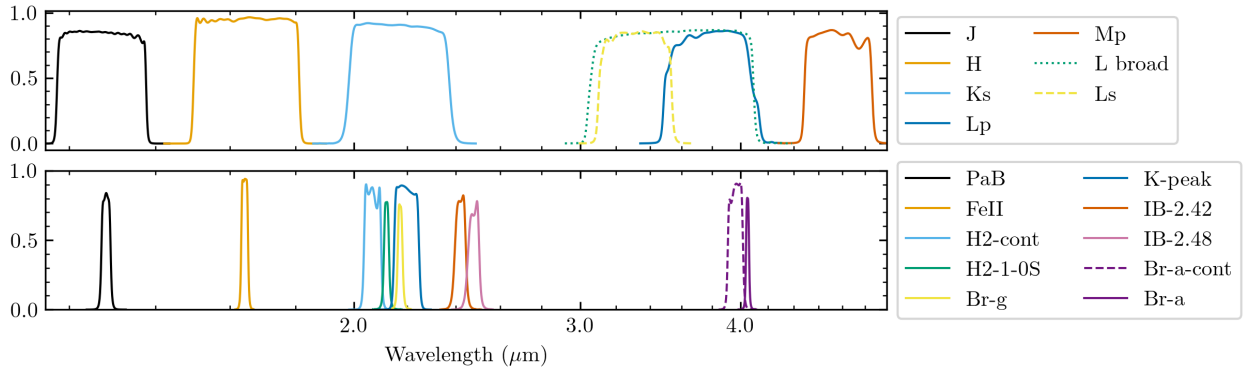
Figure 6: ERIS/NIX filters. The top row broad band filters, for which most have standard star zeropoints, and the bottom row narrow band filters whose zeropoints are deduced from their overlap with the nearest broad band filter.

We assume that the difference in zeropoint (ZP) between two filter sets is entirely due to the ratio of the integrated area of each filter:

$$ZP_2 = ZP_1 + \Delta m$$

$$\Delta m = (m_1 - m_2) = -2.5\log_{10}(f_1/f_2)$$

$$\text{Assuming: } f_1/f_2 \simeq \text{filter\_area}_1/\text{filter\_area}_2 = A_1/A_2$$

$$\Rightarrow \quad ZP_2 \simeq ZP_1 - 2.5\log_{10}(A_1/A_2)$$

These values are summarised in table 3 below.
Of course, we should account for the flux distribution of the source. A future project will convolve the standard star spectral energy distribution with the two filter sets and the zeropoint values will be refined.

Photometric Default Values for ERIS/NIX

Filter	λ_c (µm)	FWHM (µm)	average transmission (%)	peak transmission (%)	based on N_{std}	integrated area ratio	default ZP *
J	1.28	0.20	82	86	272	–	25.129 +/- 0.15
H	1.66	0.31	93	97	299	–	25.320 +/- 0.10
Ks	2.18	0.39	87	92	278	–	24.626 +/- 0.12
Short-Lp	3.32	0.43	80	86	0	Lp/Short-Lp = 1.3905	23.461 +/- 0.75
L-Broad	3.57	1.04	83	87	0	Lp/L-Broad = 0.5628	24.443 +/- 0.75
Lp	3.79	0.60	78	86	40	–	23.819 +/- 0.25
Mp	4.78	0.58	80	87	15	–	23.266 +/- 0.39
Pa-b	1.282	0.021	75	83	0	J/Pa-b = 9.4105	22.704 +/- 0.45
Fe-II	1.644	0.020	86	94	0	H/Fe-II = 14.8619	22.390 +/- 0.30
H2-cont	2.068	0.064	80	90	0	Ks/H2-cont = 6.3747	22.615 +/- 0.36
H2-1-0S	2.120	0.020	67	77	0	Ks/H2-1-0S = 20.3983	21.352 +/- 0.36
Br-g	2.172	0.020	65	75	0	Ks/Br-g = 21.3418	21.303 +/- 0.36
K-peak	2.198	0.099	83	89	0	Ks/K-peak = 4.0983	23.094 +/- 0.36
IB-2.42	2.420	0.049	71	82	0	Ks/IB-2.42 = 8.5317	22.298 +/- 0.36
IB-2.48	2.479	0.051	65	78	0	Ks/IB-2.48 = 8.9077	22.252 +/- 0.36
Br-a-cont	3.965	0.108	82	91	0	Lp/Br-a-cont = 5.1583	22.038 +/- 0.75
Br-a	4.051	0.023	69	80	0	Lp/Br-a = 24.4224	20.350 +/- 0.75

* estimated ZP values of overlap filters are given an error = 3 x ZP_{err} of parent filter   2024.02.07 M.Neeser

Table 5: A summary of ERIS/NIX default zeropoint values.